Available online at www.sciencedirect.com
SCIENCE DIRECT
Thermochimica Acta 446 (2006) 135–139
thermochimica acta
www.elsevier.com/locate/tca

Heat capacity of vitreous and crystalline $GeSe_2$ from 2 to 25 K by relaxation calorimetry

Svein Stølen*, Rune Søndenå

Department of Chemistry and Centre for Materials Science and Nanotechnology, University of Oslo, Postbox 1033 Blindern, N0315 Oslo, Norway

Received 8 January 2006; received in revised form 21 February 2006; accepted 21 February 2006
Available online 30 March 2006

Abstract

The heat capacities of vitreous and crystalline $GeSe_2$ as obtained by relaxation calorimetry from 2 to 25 K are reported. Focus is given to the effect of the structure on the heat capacities and on the boson peaks observed for both vitreous and crystalline $GeSe_2$ below 4 K. The accuracy of the commercial instrument used is considered by comparing the results obtained with earlier heat capacities determined by adiabatic calorimetry.
© 2006 Elsevier B.V. All rights reserved.

Keywords: $GeSe_2$; Heat capacity; Relaxation; Calorimetry; Boson peak

1. Introduction

Germanium diselenide is an interesting compound with a complex crystal structure in which half of the basic $GeSe_4$-tetrahedral building blocks share corners. The remaining half share edges and an open two-dimensional crystal structure results [1]. This open structure transforms to a denser three-dimensional structure well below 1 GPa on application of pressure [2,3]. In the high-pressure structure all tetrahedra share corners only. Similar changes in the intermediate-range order take place also in liquid $GeSe_2$ both as a function of pressure [4] and temperature [5,6]. This affects the properties of liquid $GeSe_2$ to a large extent. $GeSe_2$ satisfies three out of the four Zachariasen's criteria for glass formation [7] and the glass-forming ability of $GeSe_2$ is consequently good. More unusual is the variation of the viscosity of liquid $GeSe_2$ with temperature [8]. Most liquids are characterized either as strong or as fragile. In the first case the viscosity varies with temperature according to the Arrhenius equation and the short and medium range order is to a large extent the short and medium range order present in the corresponding crystalline state. Fragile liquids on the other hand show a non-Arrhenius temperature dependence of structure dependent properties like the viscosity and the local structure is here expected to be quite different from that in the crystalline state and also to vary appreciably with temperature [9,10]. While liquid $GeSe_2$ just above the glass transition temperature must be termed as a strong liquid, it is fragile above the melting temperature and a temperature induced strong to fragile transition is thus inferred [8].

$GeSe_2$ behaves anomalously in another respect as well. The heat capacity of crystalline $GeSe_2$ is higher than that of vitreous $GeSe_2$ between 12 and 60 K [11,12]. Above 60 K, the normal, opposite situation prevails and the excess heat capacity of vitreous $GeSe_2$ rises to about 39 J K^{-1} mol^{-1} at the glass transition temperature, 680 K [8]. In the present study, we extend the earlier heat capacity determinations to lower temperatures. The heat capacity of glasses typically deviates from the Debye model at low temperatures resulting in a maximum in C_p/T^3 versus temperature. The heat capacity of vitreous $GeSe_2$ is thus expected to rise above that of crystalline $GeSe_2$ as temperature is lowered. There is increasing evidence that the C_p/T^3 versus T maximum originates from the low-frequency vibrational modes giving rise to the so-called boson peak observed in Raman and neutron scattering experiments. The boson peak is basically a broad maximum in the vibrational density of states normalized by the frequency squared. These additional soft vibrations coexist with Debye-like acoustic phonon modes. In the case of vitreous silica they correspond to relative rotations of the SiO_4-tetrahedra [13]. The temperature for the maximum in C_p/T^3 takes place at

* Corresponding author.
E-mail address: svein.stolen@kjemi.uio.no (S. Stølen).

0040-6031/$ – see front matter © 2006 Elsevier B.V. All rights reserved.
doi:10.1016/j.tca.2006.02.026

around 8 and 10 K for GeO_2 and SiO_2, respectively, and even lower in temperature for B_2O_3 [14,15].

A second purpose of this paper is to test the accuracy of the heat capacity option of the Quantum Design Physical Properties measurement system (PPMS) at low temperatures. The previous data for $GeSe_2$ [11,12] were obtained by adiabatic calorimetry and the presently used relaxation calorimeter can thus be evaluated in the overlapping temperature region ($12 < T/K < 25$). Two previous studies reach quite different conclusions with regards to the accuracy and of this instrument by measurements on copper and synthetic sapphire [16,17], and a further independent comparison is warranted.

2. Experimental

2.1. Sample preparation and characterization

The starting materials used for the preparation of crystalline and vitreous $GeSe_2$ were high purity germanium (99.999%) and selenium (99.999%) from Goodfellow Inc., UK. They were mixed in stoichiometric ratio in silica glass ampoules, which were evacuated and then sealed. Crystalline $GeSe_2$ was prepared by first annealing the initial mixture at 1173 K for 48 h. The samples were subsequently ground and annealed at 923 K for 6 weeks before they were cooled to room temperature over a period of 24 h. The obtained products were examined by powder X-ray diffraction (XRD) at room temperature and were found to have the monoclinic layered structure ($P2_1/c$, $Z = 16$) [1]. No impurities could be detected by XRD or by scanning electron and optical microscopy. For producing vitreous $GeSe_2$, a sample was after the initial temperature treatment at 1173 K for 48 h dropped into a mixture of ice, NaCl, and water to quench the sample into a glassy state. The product was non-crystalline when probed by XRD and shows a glass transition at around 680 K.

2.2. Relaxation calorimetry

The heat capacity determinations were made with a fully automated relaxation calorimeter of the physical property measurement system (PPMS) from Quantum Design (QD). Here the heat capacity of the sample is determined by measuring the thermal response of a sample/calorimeter assembly to a short heat pulse. A heat-flow diagram for a standard relaxation calorimeter is shown in Fig. 1a. A relaxation calorimeter typically consists of a platform with high thermal conductivity to which a thin film heater and a temperature sensor for measuring the sample temperature are attached. The platform is connected to a heat sink via four thin wires. A schematic drawing of the calorimeter is given in Fig. 1b. The thermal link is characterized by a thermal conductance, K_1. In addition, the four wires provide electrical connections to the heater and temperature sensor. The sample with unknown heat capacity, C_x, is attached to the sample platform with high thermal conductivity grease, and the thermal link between the platform and the sample is characterized by a thermal conductance, K_2.

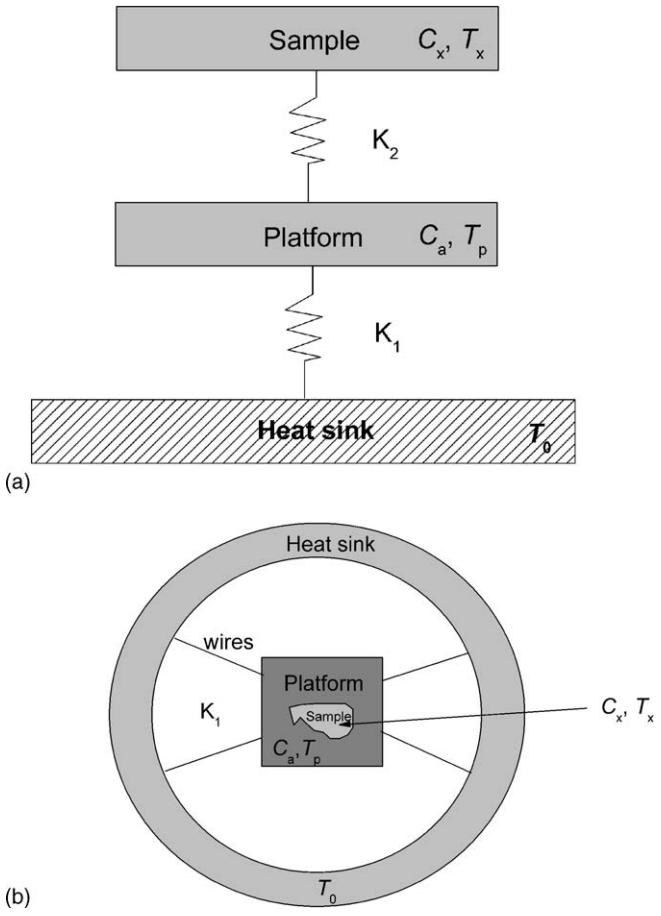

Fig. 1. (a) Heat-flow diagram for a conventional relaxation calorimeter. (b) A schematic representation of the relaxation calorimeter used.

With a power, P, applied to the platform via the thin-film heater, the coupled differential equations

$$P = C_a \frac{dT_p}{dt} + K_2(T_p - T_x) + K_1(T_p - T_0),$$
$$0 = C_x \frac{dT_x}{dt} + K_2(T_x - T_p) \quad (1)$$

describe the heat-balance condition for the system given in Fig. 1. In Eq. (1), C_a is the addenda heat capacity with contributions from the platform, the temperature sensor, the heater, and the thermal-contact grease. T_0, T_p and T_x are the temperatures of the heat sink, the platform and the sample, respectively. A power P applied to the heater warms the platform/sample assembly from T_0 to $T_0 + \Delta T$, where $\Delta T = P/K_1$. When the thermal connection between the sample and platform is very strong ($K_2 \gg K_1$), the temperature of the sample is close to identical to the temperature of the platform and in such cases the heat-balance condition simplifies to

$$P = (C_a + C_x)\frac{dT_p}{dt} + K_1(T_p - T_0) \quad (2)$$

After the heat pulse, the platform/sample assembly will cool to the heat sink temperature, T_0, according to

$$T_p(t) = T_0 + \Delta T \exp\left(\frac{-t}{\tau}\right) \quad (3)$$

where the time constant τ is $(C_x + C_a)/K_1$. As long as ΔT is small, the temperature-dependence of C_x, C_a, and K_1 can be ignored and Eq. (3) can be used to determine C_x from a measured τ. K_1 is determined by measuring the temperature change, ΔT, that results when power, P, is applied, while the addenda heat capacity, C_a, can be determined from a decay measurement with no sample attached to the platform (the thermal grease is present).

Often the sample-platform thermal link is not sufficient to insure $K_2 \gg K_1$. Then $T_x \neq T_p$ and the thermal decay is described by

$$T_p(t) = T_0 + A \exp\left(-\frac{t}{\tau_1}\right) + B \exp\left(-\frac{t}{\tau_2}\right). \quad (4)$$

2.3. The PPMS relaxation calorimeter

In the PPMS relaxation calorimeter, the platform is an alumina square with dimensions 3 mm × 3 mm. Ceramic Cernox resistance thermometers (Lakeshore Cryotronics) [18] calibrated on the ITS-90 scale are used as sample thermometer and for system control. Apiezon™ N grease is used to fix the sample to the platform. A special curve-fitting method is used to determine the heat capacity of the sample [19]. A number of heat pulses are carried out at each temperature and averaged. In order to insure accurate heat capacity data, the samples should be large enough. The lowest sample mass that can be used for a given compound is determined by the compound's electronic heat capacity, Debye temperature, and density.

3. Results and discussion

The heat capacities of crystalline and vitreous $GeSe_2$ in the temperature region from 2 to 25 K are given in Fig. 2. Two samples of significantly different mass are examined both for crystalline and vitreous $GeSe_2$. The results are shown using two different representations. The logarithmic plot in Fig. 2a enhances the presentation of the low temperature measurements while the linear plot in Fig. 2b, shows the agreement with earlier data for higher temperatures, obtained by adiabatic calorimetry [11,12].

The heat capacity of vitreous $GeSe_2$ is lower than that of crystalline $GeSe_2$ from 60 K [12] and down to about 12 K. This somewhat unusual feature must be seen in light of previous data for other glass-forming compounds. For network-forming oxides, a correlation between the difference in the heat capacity of crystal and glass and the difference in density is suggested [15]. A lower density appears to give a higher heat capacity. Thus, vitreous B_2O_3 and GeO_2 have higher heat capacities than the corresponding, denser crystalline modifications, and stishovite with a much larger density than vitreous SiO_2 has a much lower heat capacity. The situation is slightly different when crystal and glass have similar densities. Cristobalite, with a density approximately equal to (or slightly higher) that of glassy SiO_2 ($\rho = 2.2\ g\ cm^{-3}$) has a higher heat capacity than the vitreous analog. The density of vitreous $GeSe_2$ is in two studies reported to be $4.39\ g\ cm^{-3}$ [20] and $4.34\ g\ cm^{-3}$ [21], respectively, and thus to be approximately equal to the density of crystalline $GeSe_2$ ($4.39\ g\ cm^{-3}$) [1]. In analogy with the cristobalite/vitreous SiO_2-case, crystalline $GeSe_2$ has a higher heat capacity than vitreous $GeSe_2$ from 12 to 60 K. Complementary lattice dynamics calculations are needed to explain this feature microscopically.

The heat capacity data are replotted in Fig. 3 to give focus to the so-called boson peak at low temperatures. In line with the

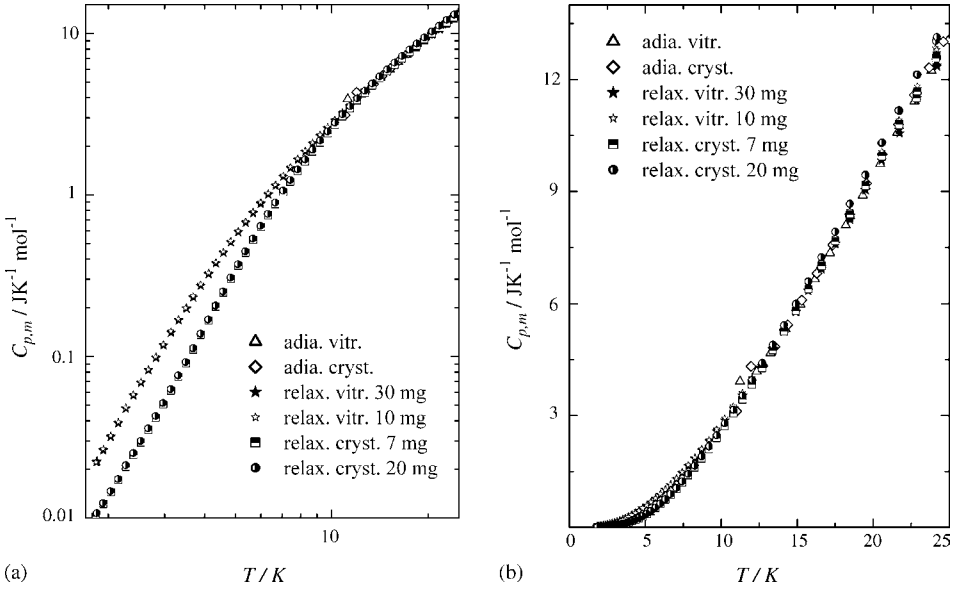

Fig. 2. Heat capacity of vitreous and crystalline $GeSe_2$ vs. temperature, (a) a logarithmic plot; (b) a linear plot. The adiabatic data for vitreous and crystalline $GeSe_2$ are taken from Atake et al. [11] and Stølen et al. [12], respectively.

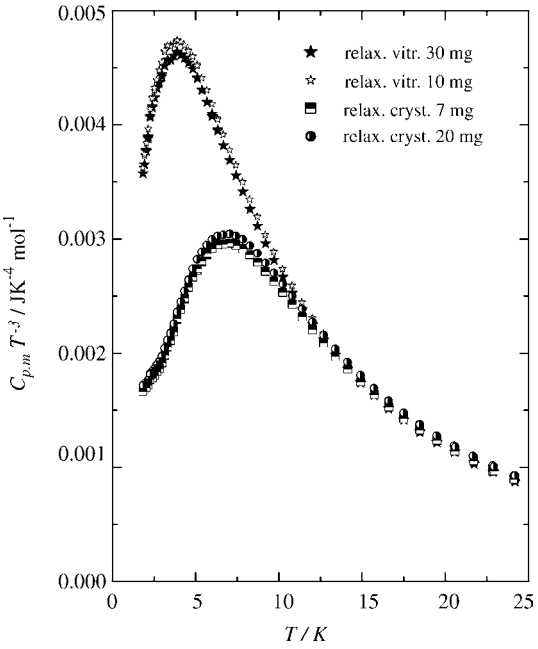

Fig. 3. $C_{p,m}/T^3$ vs. temperature.

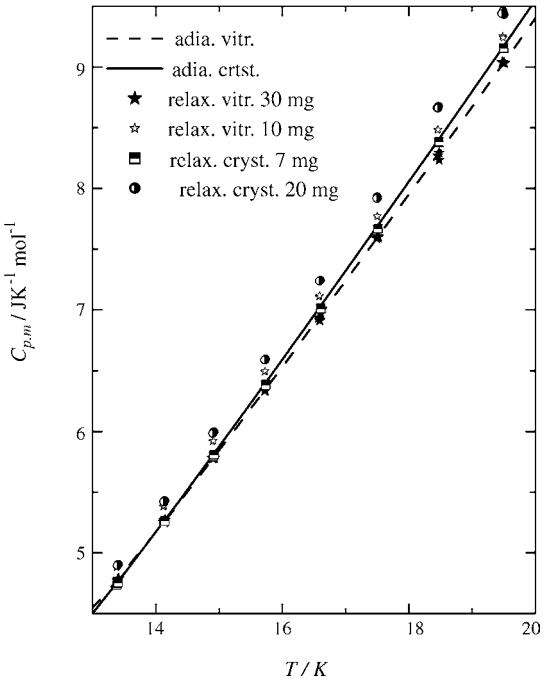

Fig. 4. Comparison of data obtained by adiabatic calorimetry [11,12] and by relaxation calorimetry.

earlier reported qualitative correlation between the boson peak and the average bond strength of the glasses as characterized by the glass transition temperature [15], the peak in C_p/T^3 versus temperature is for $GeSe_2$ (T_g = 680 K) at around 4 K. A similar boson peak temperature is observed for vitreous B_2O_3 with T_g = 540 K while vitreous GeO_2 and SiO_2, with glass transition temperatures of 980 and 1480 K, have boson peaks at approximately 8 and 10 K, respectively [14,15].

The size of the C_p/T^3 versus temperature anomaly is believed to relate to low-frequency floppy vibrational modes which involve relative rotations of rigid tetrahedral units. The density of such modes and thus the size of the anomaly are in general observed to increase with decreasing density [15]. The fact that a boson peak is also observed for crystalline $GeSe_2$ is not unexpected since its density is similar to that of the glass. Furthermore, similar boson peaks have earlier been reported for other low-density crystalline substances with open three-dimensional tetrahedral network structures. Cristobalite is again our example having a larger boson peak than the corresponding glass [15]. Crystalline compounds with high density, like B_2O_3, tetragonal GeO_2 and stishovite (the latter two contain six-coordinated Ge and Si, respectively) do not show boson-like anomalies. These general observations can be interpreted using Phillips' constraint theory in which the glass/crystal is described as a network with rigidity characterized by the ratio between the number of degrees of freedom and the number of bonding constraints [22,23]. Underconstrained systems show a high density of floppy modes, while the boson peak is small for more constrained rigid structures [24]. For our examples, the limited number of constraints for the tetrahedral network structures gives a high density of floppy vibrational modes. The larger number of constraints induced by octahedral coordination in tetragonal GeO_2 and stishovite result in rigid structures and few floppy modes [15]. Thus in general larger boson peaks are expected for network structures with lower densities. In the present case the density of crystalline and vitreous $GeSe_2$ is similar. We propose that the lower boson peak for crystalline $GeSe_2$ relates to the reduced number of degrees of freedom caused by the presence of edge-sharing tetrahedra in the crystalline state. Edge-sharing tetrahedra are less probable in the glass since large changes in the medium range order of liquid $GeSe_2$ is observed as a function of temperature [5].

The present results are compared with previous data for $GeSe_2$ obtained by adiabatic calorimetry in Fig. 4. The presumably more accurate adiabatic heat capacity measurements are shown as lines. In the overlapping range from 12 to 25 K all data obtained by relaxation calorimetry are within 3–4% of the adiabatic data used as a reference. The agreement between the two series for each sample is very good at the lowest temperatures, but less satisfying at higher temperatures. Previous studies discussing the accuracy of the Quantum Design relaxation calorimeter show both impressive and discouraging results. The results obtained for copper were within 0.75% of the recommended data for temperatures above 30 K, within 1.5% for ($30 > T/K > 4$), rising to 4% below 4 K [16]. A much larger inaccuracy was reported for synthetic sapphire. Here the data were reported to be within 5% above 100 K and increasing to 40% below 10 K. The reason was claimed to relate to the high Debye temperature and the absence of electronic contributions at the lowest temperatures which together with a low density gives a rather small heat capacity contribution from the sample [16]. A more recent study indicates a much higher accuracy, comparable to low-temperature adiabatic calorimetry. They report that the heat capacity of single crystals or sintered pellets of a range of synthetic minerals deviates from adiabatic data by a maximum of $0.5 \pm 0.8\%$ in the temperature range 100–300 K. Below

100 K the inaccuracy rises to about 2% [17]. The present results are less accurate than the data reported earlier for copper, but much more accurate than those for synthetic sapphire [16].

Acknowledgement

The project has received support from Norges Forskningsråd.

References

[1] G. Dittmar, H. Schäfer, Acta Crystallogr. B 32 (1976) 2726.
[2] T. Grande, M. Ishii, M. Akaishi, S. Aasland, H. Fjellvåg, S. Stølen, J. Solid State Chem. 145 (1999) 167.
[3] A. Grzechnik, S. Stølen, E. Bakken, T. Grande, M. Mezouar, J. Solid State Chem. 150 (2000) 121.
[4] W.A. Crichton, M. Mezouar, T. Grande, S. Stølen, A. Grzechnik, Nature 414 (2001) 622.
[5] P.S. Salmon, I. Petri, J. Phys.: Condens. Matter 15 (2003) S1509.
[6] P.S. Salmon, R.A. Martin, P.E. Mason, G.J. Cuello, Nature 435 (2005) 75.
[7] W.H. Zachariasen, J. Am. Chem. Soc. 65 (1932) 3841.
[8] S. Stølen, T. Grande, H.B. Johnsen, Phys. Chem. Chem. Phys. 4 (2002) 3396.
[9] C.A. Angell, Science 267 (1995) 1924.
[10] M. Tatsumisago, B.L. Halfpap, J.L. Green, S.M. Lindsay, C.A. Angell, Phys. Rev. Lett. 64 (1990) 1549.
[11] T. Atake, R. Abe, K. Honda, H. Kawaji, H.B. Johnsen, S. Stølen, J. Phys. Chem. Solids 61 (2000) 1373.
[12] S. Stølen, H.B. Johnsen, R. Abe, T. Atake, T. Grande, J. Chem. Thermodyn. 31 (1999) 465.
[13] U. Buchenau, M. Prager, N. Nücker, A.J. Dianoux, N. Ahmad, W.A. Phillips, Phys. Rev. B 34 (1986) 5665.
[14] R.C. Zeller, R.O. Pohl, Phys. Rev. B 4 (1971) 2029.
[15] P. Richet, D. de Ligny, E.F. Westrum Jr., J. Non-cryst. Solids 315 (2003) 20.
[16] J.C. Lashley, M.F. Hundley, A. Migliori, J.L. Sarrao, P.G. Pagliuso, T.W. Darling, M. Jaime, J.C. Cooley, W.L. Hults, L. Morales, D.J. Thoma, J.L. Smith, J. Boerio-Goates, B.F. Woodfield, G.R. Stewart, R.A. Fisher, N.E. Phillips, Cryogenics 43 (2003) 369.
[17] E. Dachs, C. Bertoldi, Eur. J. Mineral. 17 (2005) 251.
[18] B.L. Brandt, D.W. Liu, L.G. Rubin, Rev. Sci. Instrum. 70 (1999) 104.
[19] J.S. Hwang, K.J. Lin, C. Tien, Rev. Sci. Instrum. 68 (1997) 94.
[20] P. Vashishta, R.K. Kalia, I. Ebbsjö, Phys. Rev. B 39 (1989) 6034.
[21] V.S. Vassilev, S.V. Boycheva, Z.G. Ivanova, J. Mat. Sci. Lett. 17 (1998) 2007.
[22] J.C. Phillips, J. Non-cryst. Solids 34 (1979) 153.
[23] J.C. Phillips, J. Phys.: Condens. Matter 16 (2004) S5065.
[24] W.A. Kamitakahara, R.L. Cappelletti, P. Boolchand, B. Halfpap, F. Gompf, D.A. Neumann, H. Mutka, Phys. Rev. B 44 (1991) 94.